PNAS
www.pnas.org

Supplementary Information for

Early postnatal behavioral, cellular and molecular changes in models of Huntington disease are reversible by HDAC inhibition

Florian A. Siebzehnrübl*, Kerstin A. Raber*, Yvonne K. Urbach, Anja Schulze-Krebs, Fabio Canneva, Sandra Moceri, Johanna Habermeyer, Dalila Achoui, Bhavana Gupta, Dennis A. Steindler, Michael Stephan, Hoa Nguyen, Michael Bonin, Olaf Riess, Andreas Bauer, Ludwig Aigner, Sebastien Couillard-Despres, Martin Arce Paucar, Per Svenningsson, Alexander Osmand, Alexander Andreew, Claus Zabel, Andreas Weiss, Rainer Kuhn, San Moussaoui, Ines Blockx, Annemie Van der Linden, Rachel Y. Cheong, Laurent Roybon, Åsa Petersén, and Stephan von Hörsten

Correspondence to: Stephan von Hörsten
Email: Stephan.v.Hoersten@fau.de

This PDF file includes:

Other supplementary materials for this manuscript include the following:

www.pnas.org/cgi/doi/10.1073/pnas.1807962115

Supplementary Methods

RNA preparation and microarray analysis

Isolation of RNA from whole rat brain was performed using RNAeasy® Kit (Qiagen, Germany) according to the manufacturer's conditions and processed as previously described(1). Labeled, fragmented cRNA (15 µg) was hybridized to a GeneChip Rat Genome 230 2.0 Array (Affymetrix) as previously described (1). In total, 12 cRNA samples were analyzed (whole brain from three wild type control P10 pups and three homozygous transgenic P10 pups and striatum from three wild type control P10 pups and three homozygous transgenic P10 pups). For analyses, signals were first filtered for an absolute change in signal level of 1.5-fold. The remaining transcripts were subjected to statistical analysis using a T-test. Transcripts with a fold change of 1.5 and a p-value<0.05 were considered as statistically significant regulated. Categorization was based on the netAffx annotations (https://www.affymetrix.com/analysis/netaffx/index.affx). Affected gene regulation networks were determined using Ingenuity pathways analysis software (Ingenuity® systems, www.ingenuity.com).

qRT-PCR

Transcript levels of behavior-associated genes identified in gene array studies and genes involved in dopaminergic processes in the striatum were analyzed by quantitative real-time PCR as described previously (2). Primer sequences are presented in Table S1.

Receptor Autoradiography

Samples were collected and processed as described previously (3). Briefly, whole brains were rapidly removed and snap-frozen. Cryostat sections were stained for receptors of interest, placed on phosphor imaging plates (Raytest-Fuji, Straubenhardt, Germany) along with industrial tritium activity standards (Amersham Biosciences, Freiburg, Germany). Exposed imaging plates were scanned with a high-performance imaging plate reader (Raytest- Fuji). Digital receptor autoradiographs were processed using AIDA 2.31 (Raytest-Fuji).

Proteomic analysis

Samples were collected and processed as described (4). Briefly, total protein extracts from tgHD and WT P10 striata were separated using 2-DE. Protein spot patterns were evaluated using Delta2D imaging software (DECODON, Greifswald, Germany). Relative spot volume intensities were used for quantitative protein expression analysis. Data sets were analyzed using Student's *t* test. Protein spots of interest were excised from 2-D gels, trypsin-digested in gel, and fragments were analyzed by nanoflow HPLC (Dionex/LC Packings, Amsterdam, Netherlands)/ESI-MS and -MS/MS on an LCQ Deca XP ion trap instrument (Thermo Finnigan, Waltham, MA). To investigate an enrichment of specific pathways in the altered protein expression data set, we used the "Web-based gene set analysis toolkit" (WEBGESTALT) tool supplied by Vanderbilt University.

Western Blot

Dissected brain samples were snap-frozen and processed as previously described (5). Briefly, the samples were sonicated in 1% SDS and boiled for 10 min. 25 µg of each sample was separated by SDS-PAGE using a 12% running gel and transferred to an Immobilon-P transfer membrane (Millipore). The membranes were incubated for 1 h at room temperature with 5% (w/v) dry milk in TBS-Tween 20 containing the following antibodies: against Ser^{845}-GluR1, Ser^{897}-NR1, Ser^{1303}-NR2B, Ser^{19} and Ser^{31}-TH, Thr^{34}-DARPP-32, Thr^{75}-DARPP-32, against total GluR1, NR1, NR2B, NR2C, TH, CDK5 and DARPP-32 (Cell Signaling Technology, Danvers, USA). Membranes were washed three times and incubated with secondary HRP anti-rabbit antibody for 1 h at room temperature. Membranes were washed six times with TBS-Tween 20 and immunoreactive bands were detected by chemiluminescence using ECL reagents (Perkin Elmer). The autoradiograms were scanned and quantified using NIH Image 1.63 software. Levels of phosphorylated proteins were normalized to total (phosphorylated and non-phosphorylated) levels. The data were analyzed with two-tailed unpaired Student's *T*-test to evaluate statistical differences.

MRI

MRI acquisition

Diffusion weighted (DW) Imaging was performed on a horizontal 9.4 Tesla MR system (Biospec 94/20 USR, Bruker Biospin, Germany) and was acquired with a 4-shot spin-echo EPI sequence (orientation invariant icosahedral encoding scheme with 15 directions and 7 diffusion sensitization or b-values (400 - 2800 s/mm^2)). Additional image parameters were: image orientation = axial, TR/TE = 3000 ms/25 ms, diffusion gradient pulse duration (δ) = 5 ms, diffusion gradient separation (Δ) = 12 ms, NEX = 4, acquisition matrix = 128 x 128, slice thickness = 1 mm, number of slices = 18, in plane spatial resolution of 0.154 x 0.154 mm^2 (6).

MRI processing

The calculations of the invariant diffusion parametric maps, was done using custom written Matlab routines (The Mathworks, Natick, Massachusetts, USA). Standard diffusion metrics, including the three eigenvalues, mean diffusivity (MD), radial diffusivity (RD) and fractional anisotropy (FA) were calculated (7).

MRI analyses

Regions of interest (ROI) (Caudate Putamen) were manually defined on each individual and T_2 anatomical image and parametric maps (MD and FA), generated using AMIRA software (AMIRA; Template Graphics). The definition of the ROI was based on a rat brain atlas (8) and was done by a single examiner as previously described (9).

tgHD neurosphere culture

tgHD rat pups and wild type littermates were sacrificed at postnatal day 10, their brains removed and a single cell suspension prepared, cultured and maintained as described previously (10). Neurospheres after passage 2 were used for subsequent experiments. For differentiation experiments, spheres were dissociated using Accutase (PAA, Cölbe, Germany), counted and plated at 50,000 cells/ml on laminin/poly-L-ornithine (Sigma) coated coverslips. Differentiation was induced in N2 medium containing 10% fetal calf serum (Atlanta Biologicals, Lawrenceville, GA) and no mitogens. Each differentiation experiment was performed in triplicate. Some cultures were treated with different concentrations of LBH589 one hour after plating. In these cultures, medium was changed 24 hours after treatment. At various time points after plating, differentiated cultures were fixed with 4% paraformaldehyde in PBS (Sigma), washed and immunostained.

Immunocytochemistry

Fluorescence immunostaining was performed as described (10). The following primary antibodies were used: mouse anti beta III tubulin (TuJ, 1:1000, Promega), mouse anti NeuN (1:500, Chemicon), rabbit anti Darpp32 (1:500, Epitomics), rabbit anti GFAP (1:1,000, Dako), mouse anti GFAP (1:500, Sigma), mouse anti CNPase (1:100, Chemicon). Appropriate secondary antibodies were used. No signal was detected when omitting primary antibodies. Hoechst33342 (Invitrogen) was used for nuclear counterstaining. Images were taken from 10 random visual fields per coverslip on an Olympus IX-81 microscope equipped with a CCD camera. Images were imported in ImageJ and numbers of total cells (nuclei) and positively stained cells were manually counted. Only cells with neuronal morphology (compact nucleus and cell body with one prominent process longer than others) and marker expression were counted as neurons.

E13.5 embryo-derived neurosphere generation and differentiation

Neurospheres were generated from the lateral ganglionic eminences (LGE) of E13.5 embryos that resulted from the crossing of FVB/N BACHD male mice with FVB/N female mice. Note: each embryo was treated separately. At first, the uterine horns of the timed pregnant female mice were dissected out and placed in HBSS. E13.5 embryos were separately harvested and their two LGE (one from each hemisphere) were dissected out as shown in Fig. A, in a laminar flow hood under sterile conditions. The LGE were dissociated in medium used to expand the progenitors as neurospheres, according to a standardized protocol and as previously described (11). The tail of each animal was harvested and genotyping was performed, while the neurospheres were forming. The genotyping was performed using conventional PCR using the primers for the BACHD transgene: 5'-CCGCTCAGGTTCTGCTTTTA-3' (Forward) and 5'-AGGTCGGTGCAGAGGCTCCTC-3' (Reverse). After a week of growth, the neurospheres were mechanically dissociated to form secondary neurospheres. A week later, the neurospheres were isolated, washed in PBS containing 0.4% glucose and treated with 0.05% Trypsin-EDTA (Life Technologies) and mechanically triturated to obtain a single cell suspension. The cells were then counted with a hemocytometer and seeded onto poly-L-ornithine (100 µg/ml; Sigma-Aldrich) and laminin (15 µg/ml; Invitrogen) coated 96-well plates at a density of 15,000 cells/100µl in N2 medium containing 2% (v/v) N2 supplement (Thermo Fisher), penicillin and streptomycin (50 µg/ml each;

Thermo Fisher), 2mM L-glutamine (Thermo Fisher) added to Adv. DMEM/F12 medium (Thermo Fisher) supplemented with 10% fetal bovine serum (Thermo Fisher). Each embryo-derived culture was treated with 1, 10 or 100 nM of the HDAC inhibitor, LBH589 (Novartis, Switzerland) or 0.002% DMSO alone as vehicle for control condition. One well was used for each treatment condition for each embryo (n=8 embryos/genotype/treatment group). Differentiation medium was changed 24 hours later, for a medium that did not contain any of the treatments mentioned above. Cultures were fixed seven days later with 4% paraformaldehyde and processed for immunocytochemistry.

Immunocytochemistry

Triple-label immunofluorescence for glial fibrillary acidic protein (GFAP), 2',3'-cyclic nucleotide 3'-phosphodiesterase (CNPase) and microtubule associated protein 2 (MAP2) was performed on the Day 7 mouse differentiated cultures. Cells were incubated in the primary antibody against GFAP (rabbit IgG, DAKO; 1:1,000), MAP2 (chicken IgG; Abcam; 1:1,000) and CNPase (mouse IgG; Sigma; 1:1,000) overnight at 4°C in 10% normal donkey serum and 0.1% Triton-X in PBS, followed by incubation with the appropriate secondary antibodies. DAPI counterstaining (1:10,000) was used to detect cell nuclei.

Image acquisition and quantitative analysis

Images were randomly taken from 6-8 visual fields per well using an inverted LRI-Olympus IX-73 epifluorescence microscope equipped with an OCRA-R2 camera, with the Olympus cellSens Dimension program. Images were then imported and counted using the modules *cell scoring* and *neurite outgrowth* of the MetaMorph software (Version 7.8.6.0, Molecular Devices), where the total number of GFAP, CNPase, MAP2 was quantified out of DAPI positively-stained cells, and as described by others (12, 13). The same parameters were used on all the images with the exception of that for *intensity above background level*, which was minimally adjusted between the cultures from different animals. The *intensity above background level* was not changed for all the images within the same condition. The whole analysis was carried out by an investigator blinded to the experimental groupings.

Statistical analysis

Data are expressed as fold change to the DMSO-treated group. Statistical analysis was performed using GraphPad Prism 7.0. For each measurement, mean fold change values for each genotype were compared using a one-way ANOVA with Dunnett's multiple comparisons test and a possible interaction genotype-treatment was determined using a two-way ANOVA evaluation with uncorrected Fisher's LSD to determine changes between genotype for each treatment. Statistical significance was accepted at $p<0.05$.

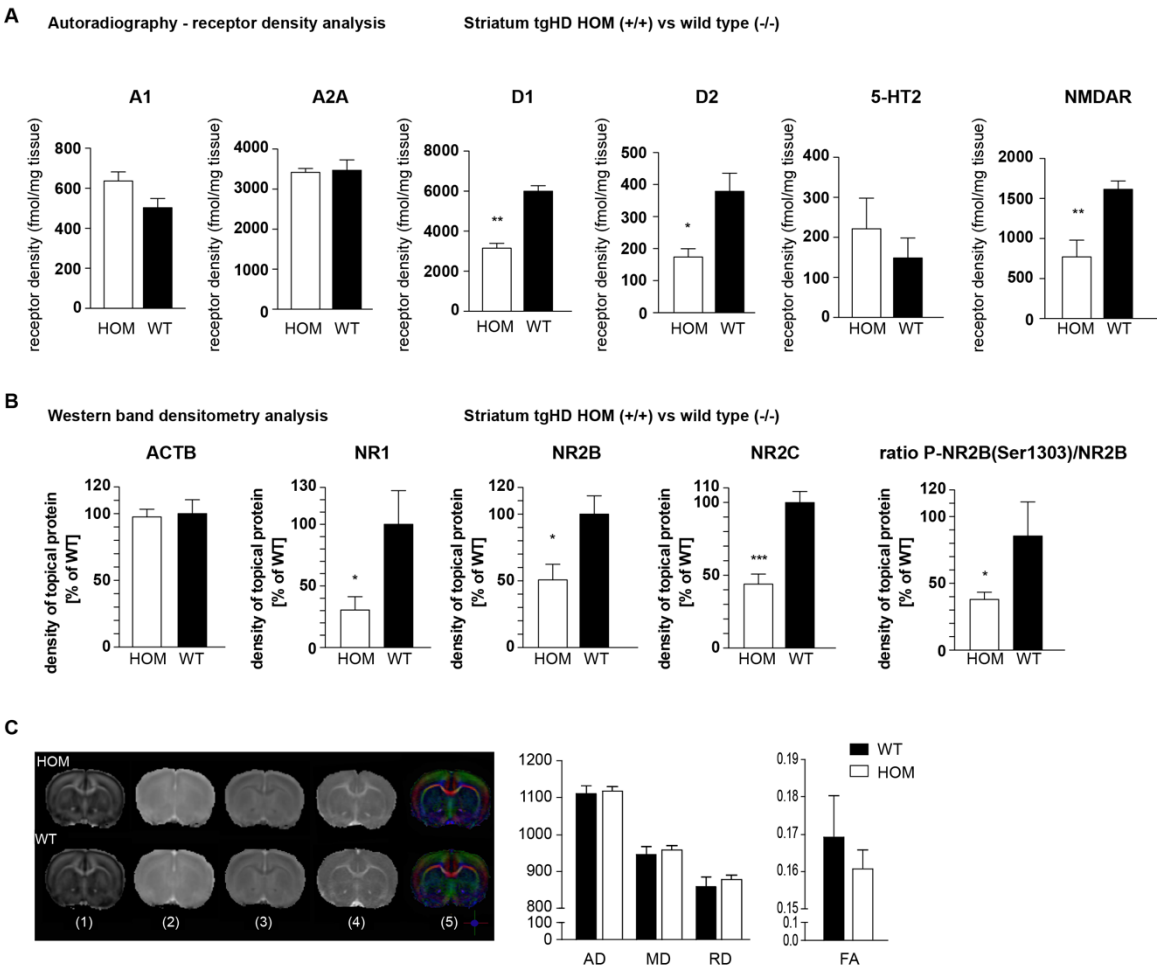

Fig. S1. (A) Receptor autoradiography data. Scintillation measurements of receptor autoradiography from P10 WT vs. tgHD pups show significant decreases in D1R, D2R and NMDAR expression, but no changes in A1, A2A and 5-HT2 receptor expression (*p<.05, **p<.01). **(B) Densitometry analysis for NMDAR expression.** Western Blot densitometry reveals significant reduction in NR1, NR2A and NR2B subunits in P10 tgHD pups over WT littermates, as well as decreased phosphorylation of NR2B (*p<.05, ***p<0.001). **(C) Diffusion-tensor MRI imaging of tgHD pups.** A single axial slice of a tgHD HOM (upper row) and WT animal (bottom) is shown (P15): (1) Fractional anisotropy (FA) map, (2) mean diffusivity (MD) map, (3) radial diffusivity (RD), (4) axial diffusivity (AD) map and (5) color encoded FEFA map. The anisotropy map discriminates white (bright regions, anisotropic) and grey matter (dark regions, isotropic). The FEFA map provides orientation of the anisotropy, which indicates the main direction of the underlying fibers (blue, caudal-rostral; red, left-right; and green, dorsal ventral). These different DT maps provide an image contrast, which facilitates the delineation of the Caudate Putamen. Different diffusion parameters were measured in the Caudate Putamen in WT versus tgHD HOM pups. Data are presented as mean and standard deviation. No statistical significance was found between both groups (AD (p = 0.563); MD (p = 0.232); RD (p = 0.121); FA (p = 0.130).

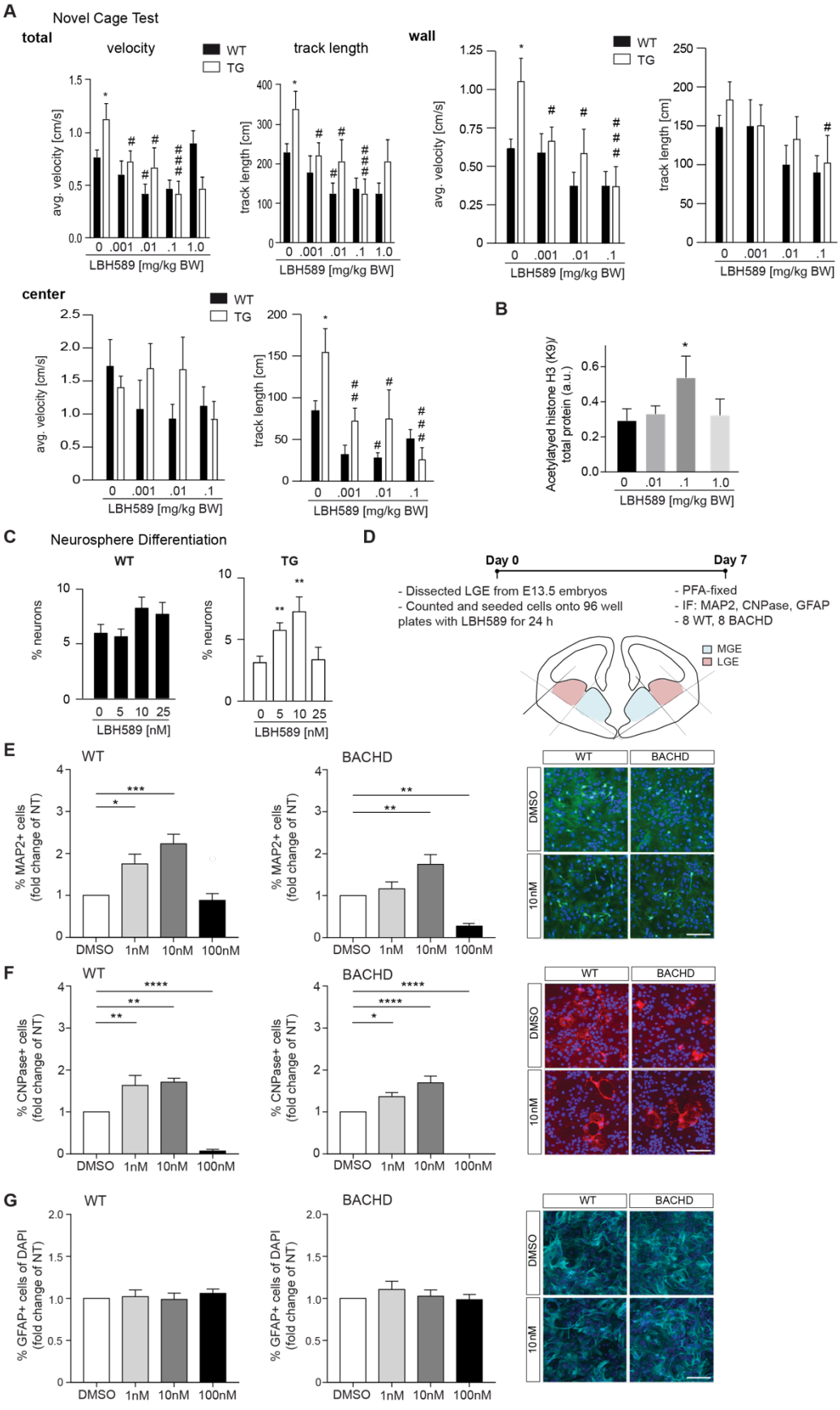
A
Novel Cage Test
total
velocity
track length
WT
TG
avg. velocity [cm/s]
track length [cm]
LBH589 [mg/kg BW]
wall
center
B
Acetylatyed histone H3 (K9)/ total protein (a.u.)
C
Neurosphere Differentiation
WT
TG
% neurons
LBH589 [nM]
D
Day 0
Day 7
- Dissected LGE from E13.5 embryos
- Counted and seeded cells onto 96 well plates with LBH589 for 24 h
- PFA-fixed
- IF: MAP2, CNPase, GFAP
- 8 WT, 8 BACHD
MGE
LGE
E
BACHD
% MAP2+ cells (fold change of NT)
DMSO
1nM
10nM
100nM
F
% CNPase+ cells (fold change of NT)
G
% GFAP+ cells of DAPI (fold change of NT)

Fig. S2. Additional LBH589 treatment data. (**A**) LBH589 treatment significantly decreased average velocity and track length in transgenic rats compared to corresponding vehicle treated transgenic animals (average velocity: 0.001 mg/kg: p=0.0194; 0.01 mg/kg: p=0.0119; 0.1 mg/kg: p<0.0001; track length: 0.001 mg/kg: p=0.0213; 0.01 mg/kg: p=0.0152; 0.1 mg/kg: p<0.0001). LBH589 had no effect on WT animals except for the 0.01mg/kg group, where average velocity and track length were significantly decreased compared to vehicle treated animals (average velocity: 0.01 mg/kg: p=0.04; track length: 0.01 mg/kg: p=0.0389). (**B**) Single dose LBH589 treatment (i.p.) increased histone H3 (K9) acetylation in the brains of rat pups at postnatal day 10. Quantitative analysis of western blots from n=3 animals, normalized to loading control (*p<0.05, one-way ANOVA). (**C**) Treatment of WT-derived, differentiating neural stem/progenitor cell cultures with increasing concentrations of LBH589 (0-25 nM) did not alter their neuronal differentiation potential significantly. Of the different LBH589 concentrations tested, the greatest induction of neuronal differentiation was observed at 10 nM (p=0.0090). (**D**) Schematic representation of the neurosphere differentiation procedure and lateral ganglionic eminence (LGE) dissection from E 13.5 BACHD embryos. (**E**) Percentage of MAP2+ neurons were significantly increased with 1nM and 10nM LBH589 in WT cultures. BACHD cultures showed increased percentage of MAP2+ neurons only with 10nM LBH589 treatment. 100nM LBH589 treatment resulted in reduced percentage of MAP2 neurons in BACHD cultures. Representative photomicrograph showing MAP2+ neurons (green) and DAPI (blue) from WT and BACHD cultures at 0 and 10 nM LBH589 treatment. (**F**) Percentage of CNPase+ oligodendrocytes were significantly increased with 1 and 10nM LBH589 in both WT and BACHD derived cultures. Representative photomicrograph showing CNPase+ oligodendrocytes (red) and DAPI (blue) from WT and BACHD cultures at 0 and 10nM LBH589 treatment. 100nM LBH589 resulted in significantly reduced CNPase+ oligodendrocytes. (**G**) No change in the percentage of GFAP+ astrocytes with 1, 10 and 100nM LBH589 treatment in both WT and BACHD cultures. Representative photomicrograph showing GFAP+ astrocytes (turquoise) and DAPI (blue) from WT and BACHD cultures at 0 and 10nM LBH589 treatment. Data represent means± SEM. Significant effects are indicated by asterisk (*p< .05, **p< .01; ***p< .001; ****p< .0001 vs NT). Scale bar corresponds to 100 μm in all images.

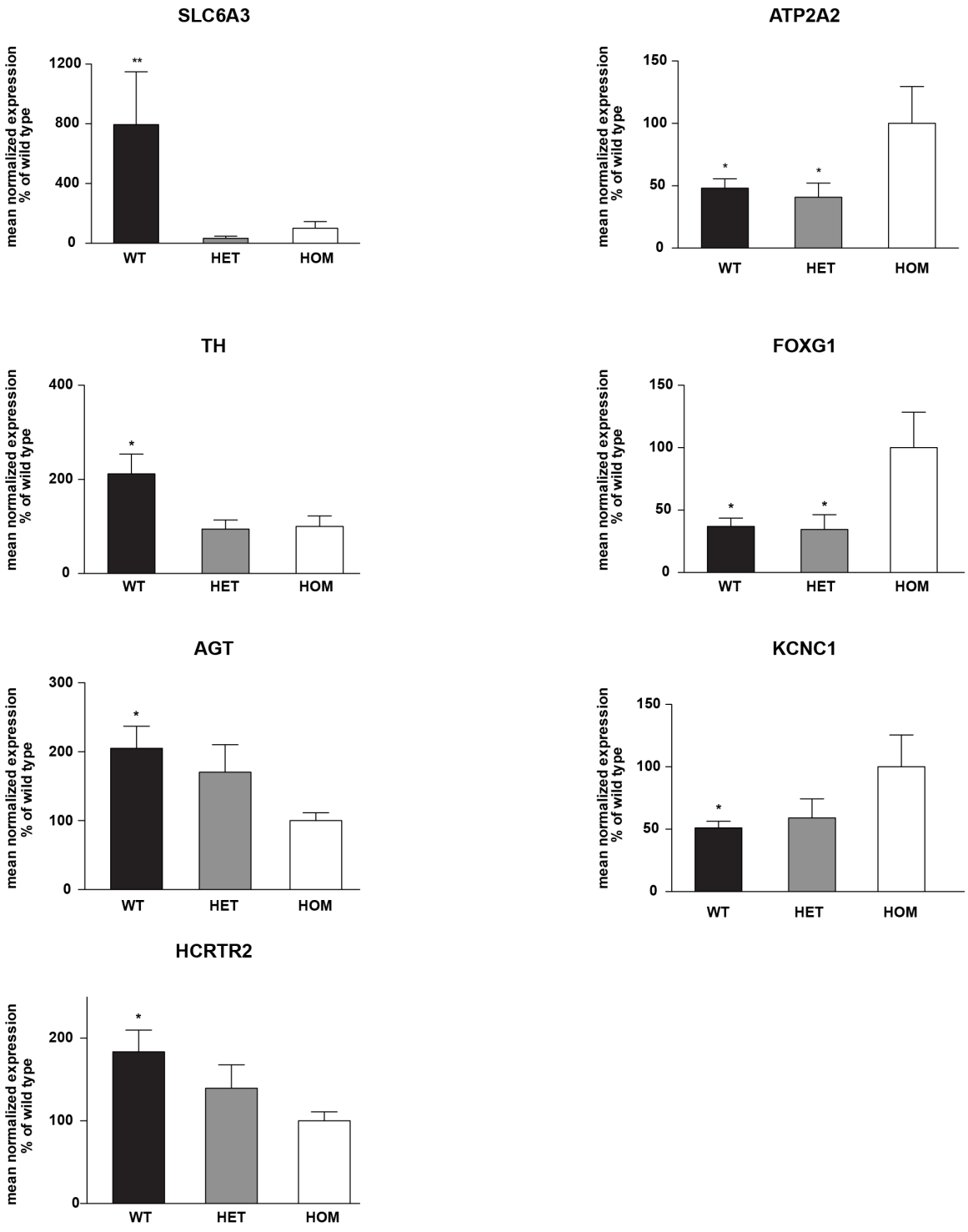

Fig. S3. Quantitative real-time PCR of HD striata. qPCR validation of transcripts SLC6A3, ATP2A2, TH, FOXG1, AGT, KCNC1, and HCRTR2 in striatal preparations of P10 tgHD pups. Significant effects are indicated by asterisk (*p< .05, **p< .01; vs HOM, ANOVA, n>6).

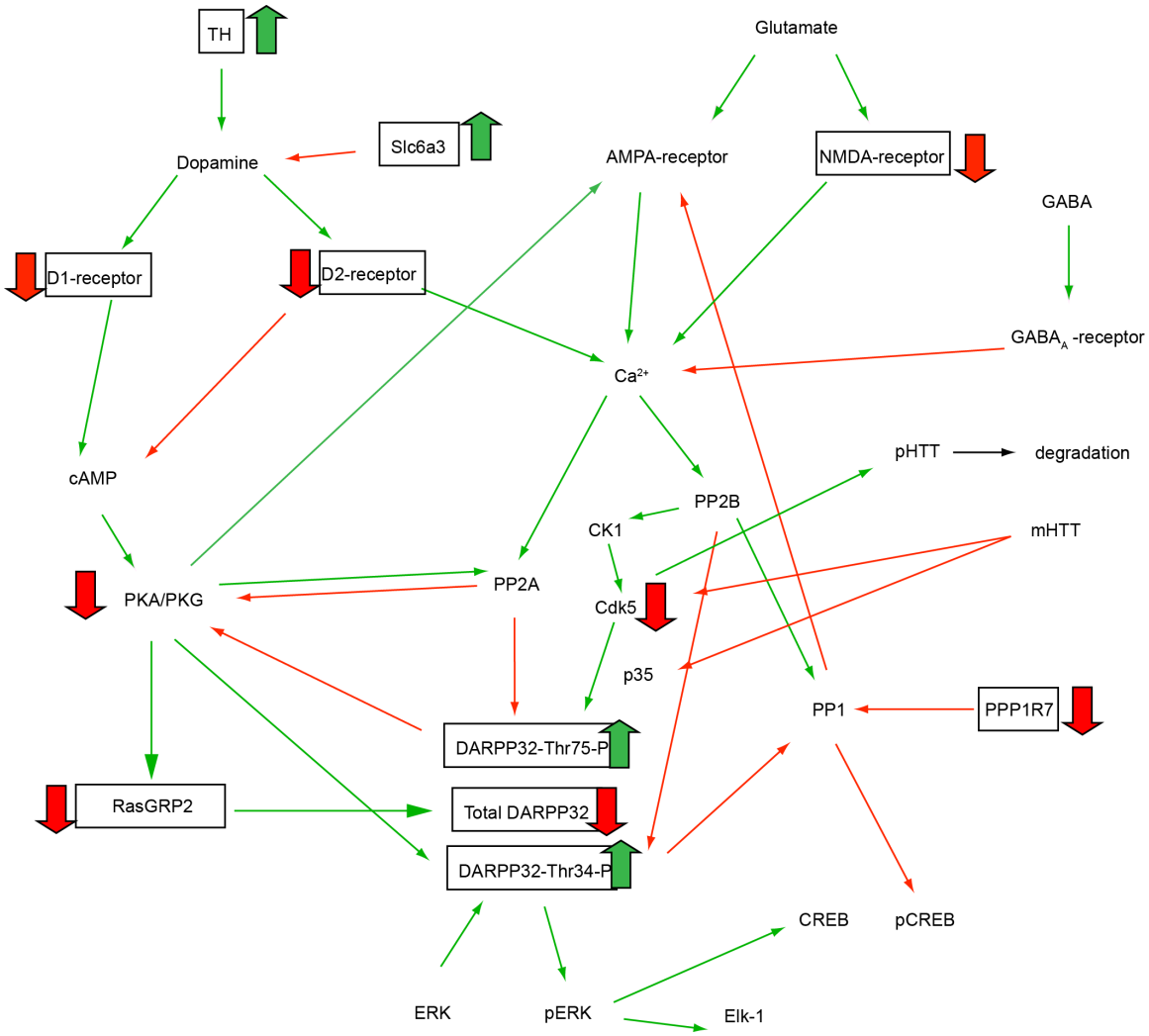

Fig. S4. Molecular alterations in early postnatal HD pups. Light green arrows indicate positive actions, while light red arrows indicate inhibitory actions. Strong red arrows indicate proteins downregulated in P10 HD pups, and strong green arrows show proteins upregulated in these animals. Black boxes indicate transcripts or proteins validated in this study.

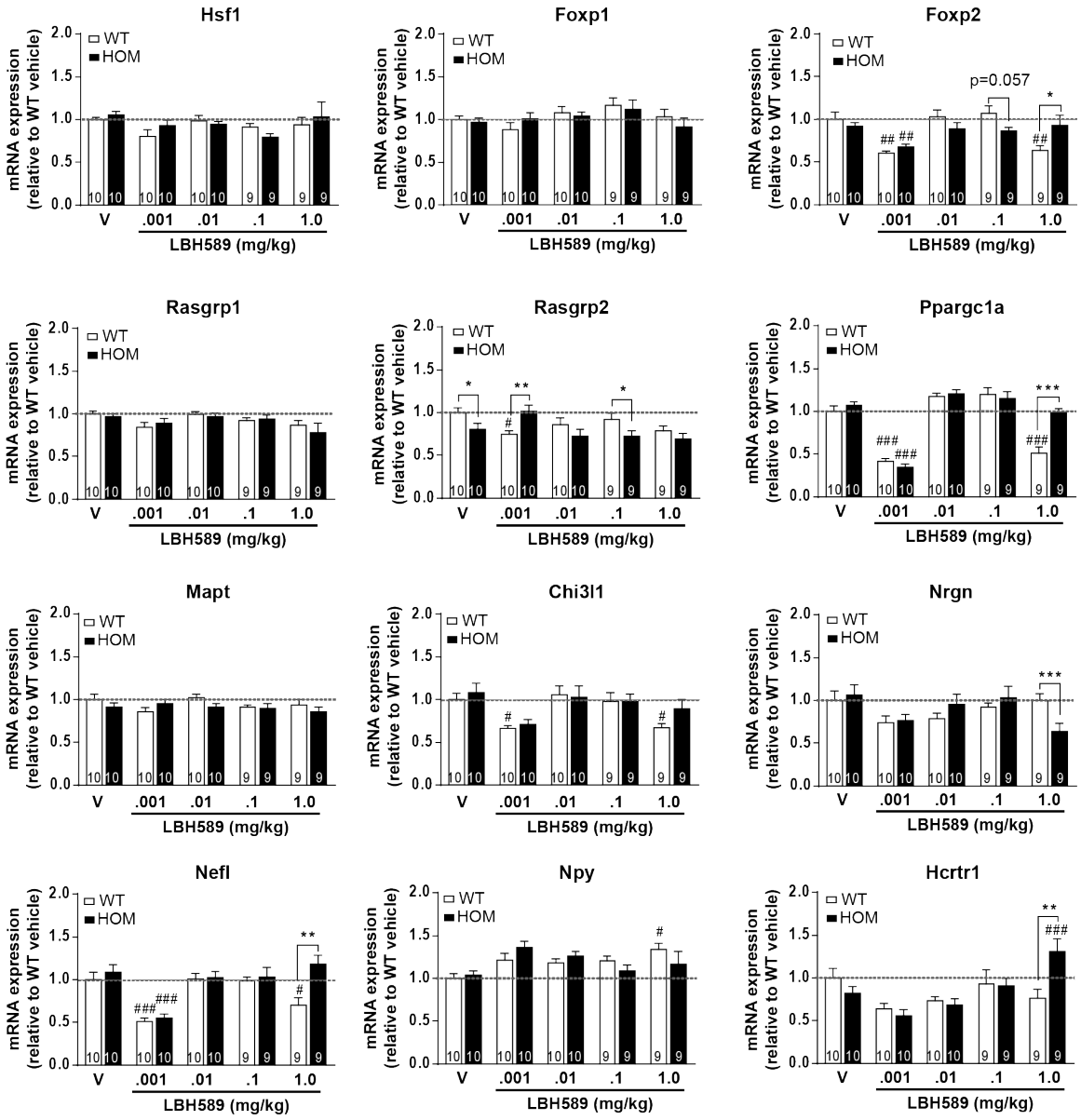

Fig. S5. **Additional transcriptional changes after LBH589 treatment.** tgHD pups were treated with vehicle (V) or different doses of LBH589 at postnatal day 8, and brain tissue was harvested at postnatal day 10. Gene expression was profiled in striatal preparations by qPCR. Numbers in bars represent number of samples for each genotype/treatment group; * represents genotype differences (compared to WT; * $p<0.05$; ** $p<0.01$; *** $p<0.001$); # represents treatment differences (compared to V; # $p<0.05$; ## $p<0.01$; ### $p<0.001$; two-way ANOVA).

Additional dataset S1 (separate file)

Microarray data of P10 WT vs tgHD rats (striatum and whole brain). The Excel spreadsheet provides descriptors, gene names and symbols, as well as p values for expression profiles of whole brain and striatal tissue of P10 WT vs. tgHD pups.

Additional dataset S2 (separate file)

Proteomic analysis of P10 striata. The Excel spreadsheet provides GI numbers, protein names, gene names, SwissProt IDs, p-values and ratios (downregulated in green, upregulated in red) for protein samples differently expressed between P10 tgHD and WT pups.

Additional dataset S3 (separate file)

PK/PD data for LBH589. The Excel spreadsheet provides dosing regimens, blood and brain levels for LBH589 in tgHD rat pups, as well as the brain/blood ratio, and mean concentrations in both tissues.

Additional data table S1

Primers and annealing temperatures used in this study.

s – sense, as - antisense

Gene	**Primer sequence (5'-3')**	**Annealing [°C]**
GAPDH_s	GATGACATCAAGAAGGTGGTGA	58
GAPDH_as	ACCAGGAAATGAGCTTCACAAT	58
AGT_s	ACACCCCTGCTACAGTCCAC	56
AGT_as	ACCCCCTCTAGTGGCAAGTT	56
ATP2A2_s	TGGAGAACGCTCACACAAAG	57
ATP2A2_as	TGCTCGATCACAAGTTCCAG	57
Cort_s	TCTGACTTTCCTTGCCTGGT	59
Cort_as	TACTTGCACGAGGAGAAGG	59
FoxG1B_s	GAACGGCAAGTACGAGAAGC	57
FoxG1B_as	TCACGAAGCACTTGTTGAGG	57
GABArb3_s	CTTGACAATCGAGTGGCTGA	56
GABArb3_as	ATTTCCAGGGTGCAGTTTTG	56
GCH1_s	GGGAAGGGTCCATATTGGTT	59
GCH1_as	ACCTCGCATGACCATACACA	59
JunB_s	ATGTGCACGAAAATGGAACA	60
JunB_as	CCTGACCCGAAAAGTAGCTG	60
HCRTR2_s	GCCTTTTCTTGCTGTCTTGG	58
HCRTR2_as	GTGAAGATGGCACTCCCTGT	58
HPRT_s	GCAGACTTTGCTTTCCTTGG	56
HPRT_as	CCGCTGTCTTTTAGGCTTTG	56
KCNC1_s	CCTGGTCTCCATCACAACCT	58
KCNC_as	ACTCCACCTTGTTGGGACAG	58
Nrg1_s	GGCACATCCATCCAAATACC	58
Nrg1_as	ACTTGGTGCAGTTTCCTGCT	58
OPRL1_s	TGAGCGTAGACCGCTATGTG	55
OPRL1_as	CATGATGGCAACAGGAACAC	55
Slc18A2_s	CCACTCTGCTTTTTCCTTCG	59
Slc18A2_as	GCGACGTTAGAGGGTCTCAG	59

Slc6A3_s	CGGAGCACTGGCTTTAGTTC	58
Slc6A3_as	ACAGGCCTGCATTTAACACC	58
TH_s	TGTGTCCGAGAGCTTCAATG	57
TH_as	GGGCTGTCCAGTACGTCAAT	57
D1A_s	CATTCTGAACCTCTGCGTGA	56
D1A_as	GTTGTCATCCTCGGTGTCCT	56
PKA_s	AGCAGGAGAGCGTGAAAGAG	58
PKA_as	GCTTCAGCTTCACCACCTTC	58
CDK5_s	GCAATGATGTGGATGACCAG	56
CDK5_as	CACGACATTCACCAAGGATG	56
DARPP32_s	ACCACCCAAAGTCGAAGAGA	56
DARPP32_as	GAGGCCTGGTTCTCACTCAG	56
Ppp3ca_s	TACACGGTGGTTTGTCTCCA	57
Ppp3ca_as	CAACCCCTGACTGTGTTGTG	57
Ppp3cb_s	ACAGGGATGTTGCCTAGTGG	56
Ppp3cb_as	TCAGTGGTATGTGCGGTGTT	56
Ppp2cb_s	TGGTGGAAAATCACCAGACA	56
Ppp2cb_as	GGCGTTCCCATACTTTCGTA	56
COMT_s	GAGCTGGGAGCTTACTGTGG	58
COMT_as	GTAGGCCTGCAAAGTTCAGC	58
FOXP1_s	CGGCCTTTCTAAAACATCTCAAC	63
FOXP1_as	TGTACTCTACATTGAGCTGTGCTTCTATC	63
FOXP2_s	TATGGAGCAGCCCTTAATGC	63
FOXP2_as	GGTTACTTAGCAAAGGCAAACTG	63
RASGRP1_s	GATGAACTGCCACAAACAGTGC	64
RASGRP1_as	TGCATGGAGCAGATCTTTGG	64
RasGRP2_s	CAAGATCCTGTTCCAGGACTATCAC	58
RasGRP2_as	ACCCACTGAGAGACACTGTTGAAG	58
HSF1_s	AGCTTCCACGTGTTTGACCAG	65
HSF1_as	AAGCTGGCCATGTTGTTGTG	65
CHI3L1_s	CTGTGCACCCATATCATCTACAGC	66
CHI3L1_as	AGTGTCTTCAGTCTGGGGTTTCTG	66
MAPT_s	GCAAGGGGAAGTCTTGAAGTGTAG	66
MAPT_as	TAGCCTTATGGCACCTCTTCTCTC	66
NEFL_s	TCGAGCATTCCCAGCCTACTATAC	66
NEFL_as	TCTTTCTCCTTCTCCTCCTCTTCTG	66
NRGN_s	TCCCGCTCTCCTTTGTTTATGC	66
NRGN_as	AAAAACCTTCCAGCCACAACCC	66
NPY_s	TCGTGTGTTTGGGCATTCTG	63
NPY_as	TTGATGTAGTGTCGCAGAGC	63
HCRTR1_s	TGGTGGTTCTGCTGGTTTTTGC	67
HCRTR1_as	TGGCGAAACATCCCAAACACTC	67
PPARGC1A_s	ACACCGCACACATCGCAATTC	66
PPARGC1A_as	TTGCTTTCTGCTTCTGCCTCTC	66

References

1. Nguyen HP, *et al.* (2008) Age-dependent gene expression profile and protein expression in a transgenic rat model of Huntington's disease. *Proteomics Clin. Appl.* 2:1638-1650.
2. Schade J, *et al.* (2008) Regulation of expression and function of dipeptidyl peptidase 4 (DP4), DP8/9, and DP10 in allergic responses of the lung in rats. *The journal of histochemistry and cytochemistry : official journal of the Histochemistry Society* 56(2):147-155.
3. Bode FJ, *et al.* (2008) Sex differences in a transgenic rat model of Huntington's disease: decreased 17beta-estradiol levels correlate with reduced numbers of DARPP32+ neurons in males. *Human molecular genetics* 17(17):2595-2609.
4. Zabel C, *et al.* (2009) A large number of protein expression changes occur early in life and precede phenotype onset in a mouse model for huntington disease. *Molecular & cellular proteomics : MCP* 8(4):720-734.
5. Qi H, *et al.* (2009) Antidepressants reverse the attenuation of the neurotrophic MEK/MAPK cascade in frontal cortex by elevated platform stress; reversal of effects on LTP is associated with GluA1 phosphorylation. *Neuropharmacology* 56(1):37-46.
6. Blockx I, *et al.* (2012) Identification and characterization of Huntington related pathology: an in vivo DKI imaging study. *NeuroImage* 63(2):653-662.
7. Basser PJ & Pierpaoli C (1996) Microstructural and physiological features of tissues elucidated by quantitative-diffusion-tensor MRI. *J Magn Reson B* 111(3):209-219.
8. Paxinos G & Watson C (1998) *The Rat Brain in Stereotaxic Coordinates* (Academic Press, San Diego).
9. Blockx I, *et al.* (2012) Microstructural changes observed with DKI in a transgenic Huntington rat model: evidence for abnormal neurodevelopment. *NeuroImage* 59(2):957-967.
10. Siebzehnrubl FA, *et al.* (2007) Histone deacetylase inhibitors increase neuronal differentiation in adult forebrain precursor cells. *Exp Brain Res* 176(4):672-678.
11. Roybon L, *et al.* (2008) Effects on differentiation of embryonic ventral midbrain progenitors by Lmx1a, Msx1, Ngn2, and Pitx3. *J Neurosci* 28(14):3644-3656.
12. Lamas NJ, *et al.* (2014) Neurotrophic requirements of human motor neurons defined using amplified and purified stem cell-derived cultures. *PLoS One* 9(10):e110324.
13. Li H, *et al.* (2016). Protein Prenylation Constitutes an Endogenous Brake on Axonal Growth. *Cell reports* 16(2):545-558.